PHYSICAL REVIEW B VOLUME 25, NUMBER 4 15 FEBRUARY 1982

Determination of bond lengths from extended x-ray absorption fine structure using the linear phase functions

Mary Beth Stearns*
Ford Research Staff, Dearborn, Michigan 48121
(Received 3 August 1981)

The extended x-ray absorption fine-structure (EXAFS) spectra of many elements and compounds have been analyzed to determine their phase functions as a function of the zero of kinetic energy, E_0, of the excited electron and the weighting power of the wave vector used in the Fourier transforms. It is found that a linear phase function exists for any material at some particular value of $E_0=E_c$. The procedure for determining this E_c value is described. A linear-phase-function method of determining bond lengths is proposed and compared to other existing methods of EXAFS bond-length determinations. The many advantages of using these linear phase functions in EXAFS analysis are discussed. With the use of the linear phase functions with a linear extrapolation of their parameters, it is demonstrated that it is possible to verify the existence of a more general form of phase transferability which relates the phase functions of different atom pairs. Such relations allow the number of phase functions needed to characterize a system of N atoms to be reduced from N^2 to $2N-1$. This type of comparison is not feasible with the usual nonlinear phase functions.

I. INTRODUCTION

The use of extended x-ray absorption fine structure (EXAFS) to obtain structural information has undergone extensive development in recent years. This has occurred because of the improvement in the quality of the data due to the increase in x-ray intensity from electron storage rings and because Lytle, Sayers, and Stern[1] advanced the analysis procedure significantly by introducing Fourier-transform techniques. Stern[2] and others[3,4] have attempted to establish a strong theoretical basis for the analysis. In particular Lee and co-workers[3,5] have calculated scattering $F(\pi,k)$ and phase-shift $\phi(k)$ functions that are often used in the analyses of data.

In evaluating coordination numbers or bond lengths in unknown materials, it is necessary to assume amplitude and phase transferability from model compounds of known structure or from calculated functions. It has now been well established[6,7] that amplitude transferability for coordination number determinations is not generally valid but holds only between "chemically similar" substances. However the transferability of phases for bond-length determinations appears to be more generally valid.

By now several procedures have been proposed to obtain bond lengths. They are all closely related and generally assume that the zero of kinetic energy, E_0, of the excited electrons is within a few volts of the K edge. In determining an unknown bond length, E_0 is treated as a free parameter and adjusted to meet certain specified criteria. This procedure hopefully compensates for many of the approximations made in the analysis. A second parameter n, the weighting power of the wave vector is also introduced in most analyses. In Secs. III and IV we investigate the effects of these two parameters and develop a new method of treating the data which determines the linear phase function of a material. We show that there are great advantages in analyzing the data using this linear phase function.

In Sec. II we describe the initial data reduction and the determination of the radial-scattering distribution. In Sec. VI a new linear method of analysis is proposed. In Sec. VII we discuss some of the other methods of analysis and their limitations. In Sec. VIII we derive and test general phase transferability.

II. GENERAL ASSUMPTIONS AND PROCEDURES

The generally used one-electron single-scattering form representing the EXAFS oscillations is given

by[2]

$$\chi(k)=-\sum_i \frac{N_i}{kr_i^2}F_i(\pi,k)e^{-2\sigma_i^2k^2} \times e^{-2r_i/\lambda_i}\sin[2kr_i+\phi_i(k)] , \quad (1)$$

where the index i indicates the ith-neighbor shell of atoms surrounding the absorbing atom. N_i is the number of atoms in the ith shell and r_i is its distance from the absorbing atom. F_i is the amplitude of the backscattering function of the atoms in the ith shell and σ_i is a correlated Debye-Waller factor. λ_i is the mean free path of the electron which has been ejected from the absorbing atom. It has a k dependence and for the first shell is due mainly to inelastic-scattering processes. We subscript λ_i since it may vary for the different shells. ϕ_i is the phase shift of the electron due to backscattering from the ith shell. It has a contribution of ϕ_a arising from the absorbing atom and a component ϕ_b arising from the backscattering atom. Equation (1) does not take into account any interference or multiple-scattering effects within or between shells. These effects as well as many-body relaxation effects have been discussed by several authors[3,4,6] and can be incorporated, to some extent, by introducing further parameters into Eq. (1).

As seen from Eq. (1), even in the one-electron single-scattering approximation to $\chi(k)$, each shell is characterized by six parameters or functions plus another parameter, E_0, which represents the zero of kinetic energy of the electrons. Due to the large number of parameters EXAFS analysis is a very intricate process which must be applied with caution. Three types of information have mainly been obtained from EXAFS data: (1) Bond-length determinations which are mainly sensitive to the phase functions of $\phi(k)$. (2) Coordination numbers, N_i, which are obtained by evaluating the prefactors of the sine functions in Eq. (1). Both of these quantities are preferably obtained from data taken at low temperatures in order to enhance the EXAFS oscillations. (3) The correlated Debye-Waller factor σ_i is obtained by varying the temperature[6,8] and will be discussed no further here.

The data analyzed here were taken at SSRL at Stanford and CHESS at Cornell. The energy resolution at both storage-ring sites is determined by a 1—2-mm slit at about 17—20 m from the storage-ring orbit. This gives about 1—2-eV resolution for 7—8-keV x rays and about 10—15 eV for 25-keV x rays. The main effect of this energy spread is to dampen the EXAFS oscillations.[9] It does not affect the nodes appreciably and so it is not necessary to deconvolute the energy resolution from the oscillations for bond-length determinations. Thus, we have not made such corrections in this analysis. Such corrections can obviously be very important for coordination number determinations.

A. Initial data reduction

The generally used procedure of data reduction of an x-ray absorption curve is similar to the following. We first find the absorption coefficient $\mu'(E)d=\ln(I/I_0)$ where I is the measured intensity of x rays of energy E. The region below the K edge is then extrapolated to higher energies by fitting it to a Victoreen formula given by

$$\mu_b(E)d=A/E^3+B/E^4 , \quad (2)$$

where A and B are determined by usual curve-fitting procedures. It is then subtracted from the measured $\mu'(E)d$ to give $\mu(E)d$. The region above the K edge is then smoothed by one of various procedures (multiple averaging, spline fitting, etc.) to obtain the absorption by isolated atoms, $\mu_0(E)d$. The oscillations χ are then obtained by taking the difference between the measured $\mu(E)d$ and $\mu_0(E)d$ and normalizing by dividing by the properly scaled atomic absorption coefficient $\mu_a(E)$ due only to the transitions of the absorbing atom. The $\mu_a(E)$ curves are well determined quantities which over the years have been tabulated in many works, e.g., see Ref. 10 where the atomic absorption due to only the K edge is essentially given by

$$\mu_a(E)=(C_1-C_2)/E^3-(D_1-D_2)/E^4 . \quad (3)$$

The C and D values are tabulated in Ref. 10.

Often the samples being measured contain many atomic species, or are mounted on some backing, or may contain holes so their exists a background due to many effects. However near an edge the observed step and oscillations should be due to only the atomic species being measured. We normalize out all other effects by finding the step value $\mu_s(E_1)d=\mu_0(E_1)d-\mu_0(E_1)d$ at some energy E_1 slightly above the K edge, (e.g., $E_1=20$ eV) and then scaling by the factor $\mu_s(E_1)d/\mu_a(E_1)$. Thus, we obtain $\chi(E)$ given by the expression

$$\chi(E)=\frac{[\mu(E)d-\mu_0(E)d]\mu_a(E_1)}{\mu_s(E_1)d\mu_a(E)} . \quad (4)$$

Next $\chi(E)$ is transformed to $\chi(k)$ by assuming

the electrons are free, i.e.,

$$k=[2m/\hbar^2(E-E_0)]^{1/2}, \tag{5}$$

where E_0 is a parameter which defines the zero of kinetic energy of the outgoing electron. It is a parametric quantity sometimes called the "inner potential." In a simple picture of a metal, the K edge corresponds to the Fermi level E_F, so E_0 would be expected to have a value similar to the bottom of the conduction band.

In another view, considering the electrons as being in free space, E_0 would correspond to the work function or in the case of a nonmetal to the ionization potential. Both pictures have been used in the literature. The values corresponding to the phases and amplitudes of Lee *et al.*[3,5] span the range around ± 8 eV. It is not at all clear that it is justified to treat E_0 as k independent but for practicality this is done. In Sec. III we examine the consequences of varying E_0 in greater detail.

B. Determination of radial-scattering distribution

The next usual step in the analysis is to take the Fourier transform (FT) of $k^n\chi(k)$. The purpose of the k^n factor is to reduce the k dependence from the prefactor of the sine function in Eq. (1). At this stage a window function $W(k)$, which falls off smoothly near the minimum and maximum k values, is also used. This suppresses the side peaks which would be caused by sharp cutoffs. In the data presented here an error function of width $=1$ Å^{-1} has been used. To further reduce cutoff effects the minimum k is always taken at a node in $\chi(k)$. The oscillations near the K edge are not used since band-structure effects dominate in this region. Thus the minimum k is generally $\gtrsim 3-4$ Å^{-1}. The radial-scattering function is thus given by

$$R(r)=-\frac{2}{\pi}\int_{k_1}^{k_2} W(k)k^n\chi(k)e^{2i\vec{k}\cdot\vec{r}}dk\ . \tag{6}$$

$\chi(k)$ and its Fourier transform $R(r)$ with $n=3$ are shown in Fig. 1 for an Fe spectrum taken at around 80 K.

III. EFFECTS OF VARIATION OF E_0 AND n

Let us investigate the effects on $R(r)$ of the two arbitrary parameters, E_0 and n, which have been introduced into the analysis.

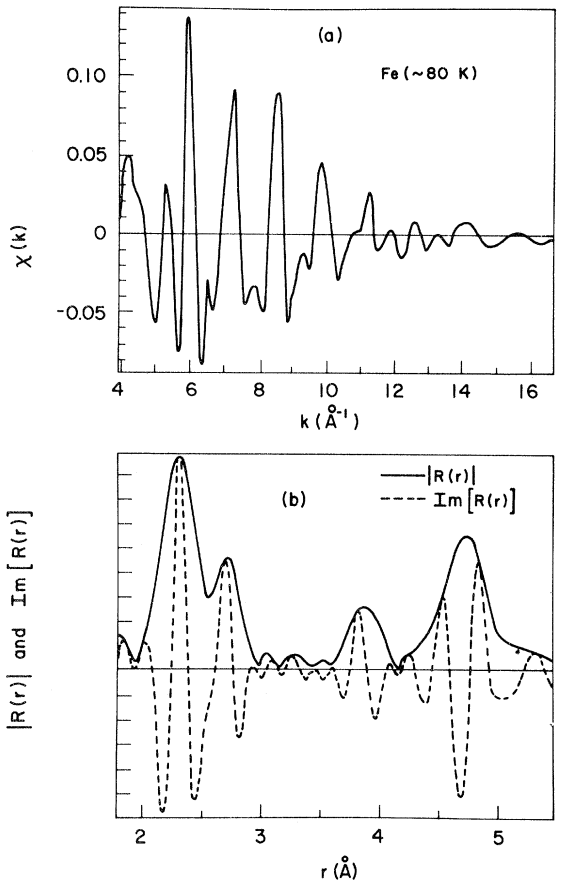

FIG. 1. (a) EXAFS oscillations $\chi(k)$ for Fe at ~ 80 K and $E_0=-32$ eV. (b) Magnitude $|R(r)|$ and imaginary Im$[R(r)]$ of the Fourier transform of $k^3\chi(k)$ for Fe.

A. Peak position behavior

In Fig. 2(a) we show the variation of the peak positions of $R(r)$ as E_0 is varied for the n values of 1, 3, and 5 for a 5-μm Ni foil at about 80 K. E_0 is measured relative to the K-edge energy which is taken as the half-height of the absorption step. The peak positions are shown for the first ($N1$), third ($N3$), and fourth ($N4$) shells surrounding the absorbing atom. We observe two striking features. One is that there exists an E_0 value that gives a transform peak shift which is independent of the weighting factor n. Let us call this crossover energy E_c. The other is that, for metals, E_c is essentially the same for all the well-resolved inner shells. This behavior is seen in all the metals examined so far. They are listed in Table I.

We can understand the general behavior of the peak-position variation in Fig. 2(a) as follows. In converting from electron kinetic energy to wave

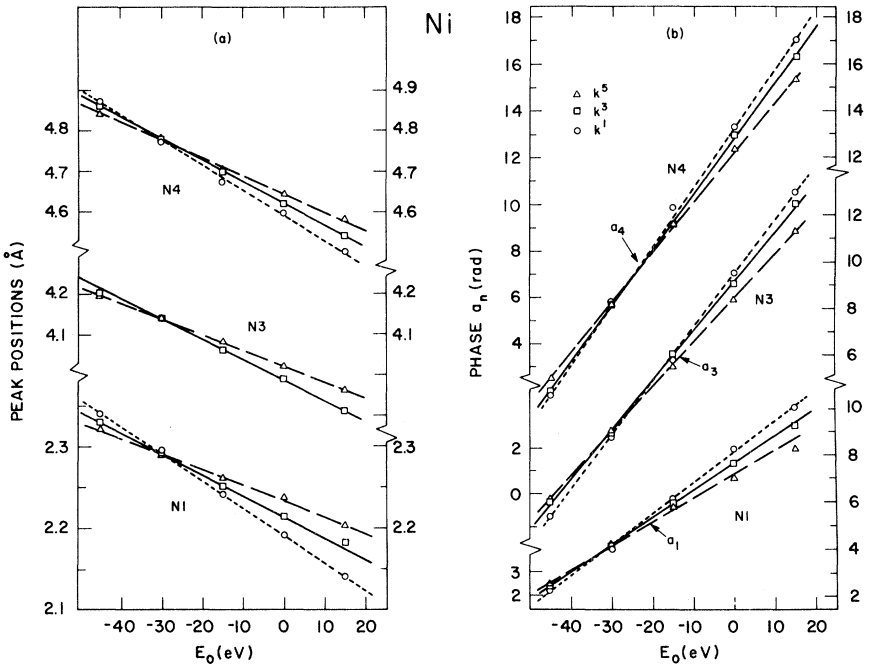

FIG. 2. (a) Peak positions of the $N1$, $N3$, and $N4$ shells of Ni as a function of E_0 for various wave-vector weighting factors, k^1, k^3, and k^5. Note the r scale for $N1$ is a factor of two larger than that for the other shells. (b) The k-independent part of the phase a_i as a function of E_0 for various weighting factors.

vector, Eq. (5), we see that a change in E_0 by ΔE results in a change in the k scale of Δk given by

$$\Delta k = m\Delta E/\hbar^2 k \ . \tag{7}$$

Thus, for a given ΔE, the k scale changes much more at small k than large k. As a result, for a shift of ΔE, the $\chi(k)$ curve is affected more at smaller k than larger k. Since for larger n the higher k values are weighted more than the lower k values, for a given ΔE, $\chi(k)$ changes less for

TABLE I. E_c and $E_{\rm LB}$ values and peak shifts for first-neighbor shells of various elements (energies are in eV and distances in Å).

Element	E_c	$E_{\rm LB}$	$-\Delta r_1$ $(=b/2)$	$-\Delta r_{\rm LB}$	$\delta r_{\rm LB}$	r_1[a]
^{26}Fe	−32	8	0.19	0.30	0.00	2.482
^{28}Ni	−29	2.5	0.20	0.28	−0.01	2.490
^{29}Cu	−24±2	5	0.20	0.29	−0.02	2.553
^{32}Ge	−26(−29)[b]	4(1)	0.20	0.27	−0.01	2.449
^{33}As	−23(−28)	3(−2)	0.21	0.28	−0.016	2.516
^{34}Se	−17(−20)	7(4)	0.23	0.28	0.006	2.374
^{41}Nb	−10	−6	0.30	0.31	−0.025	2.857
^{42}Mo	−14	−8	0.25	0.265	0.00	2.724
^{45}Rh	0	−5	0.28	0.27	−0.01	2.688
^{47}Ag	28	−1	0.38	0.29	−0.10	2.886
^{50}Sn (β)	13	0	0.37	0.32	−0.02	3.02
^{51}Sb	0	5	0.25	0.265	0.02	2.903

[a]See Ref. 11 for sources of distances.
[b]Values in parentheses are with respect to the peak above E_K.

larger n than for smaller n. Thus, the peak position derived from the Fourier transform of $\chi(k)$ shifts less for higher n than for smaller n. This is just the behavior seen in Fig. 2(a) where the higher the power of n the less the shift in the peak position variation with E_0.

The significance of the existence of an E_0 value, E_c, that gives a peak position which is the same for any weighting factor n is the following. As seen in Eq. (1) the contribution to $\chi(k)$ from a given shell is of the form

$$\chi_1(k) = -A(k)\sin(2kr_1+\phi) . \tag{8}$$

Since the FT of a sum is the sum of the FT's of the individual terms, we can consider each shell separately. As derived below [Eq. (10)], the peak position of a given shell is essentially determined by the argument of $\sin(2kr_1+\phi)$. Thus, the peak position of a given shell being independent of n (i.e., of how χ is weighted) means that all the nodes in χ_i are equally spaced in k. This only occurs if $\phi_i(k)$ is a linear function of k. Thus, $\phi(k)=a-bk$ for E_c.

The second feature of E_c being nearly the same for all the well-resolved inner shells has been found to hold only for the metals investigated so far. This can be attributed to the crystal potentials in metals being quite isotropic due to the presence of conduction electrons. Not only do the well-resolved first few shells have the same E_c values but their shifts in peak positions, Δr_i are essentially the same at E_c. This behavior is not found in nonmetals. There the E_c values as well as the peak shifts, Δr_i, are different for the different shells. For example for Ge we find the E_c values are -26, -32, and -16 eV for the $N1$, $N2$, and $N3$ shells, respectively, while the respective Δr_1 values are $r=-0.20$, -0.11, and -0.17 Å. This is as expected since the electron densities and potentials in nonmetals are anisotropic due to the directionality of the bonds in these materials.

We have found that a crossover point is obtained for all good data sets of K edges investigated so far (materials with $Z<51$). In the cases where we had a poor data set (low signal-to-noise ratio, glitches, etc.) and found no consistent crossover point, invariably when we obtained a better data set we found good, clear crossover points. Thus we assume that at least for materials containing elements with $Z<51$ there is some E_0 whose corresponding phase function is approximately linear. In Sec. IV we derive the phase functions as a function of E_0 by back-transforming and show that $\phi(k)$ is indeed linear at E_c. If $\phi(k)$ has too complex a shape there may be no linear $\phi(k)$, e.g., we have found that the Pt L transition does not give a good crossover point. Thus, the phase function for very high Z materials may have such complex shapes that they have no linear phase functions. However for the materials investigated here with $Z\leq 51$ linear phase functions do exist. In general we have found that the $\phi(k)$ functions obtained by back-transforming are less structured and have less curvature than those calculated by Teo and Lee.[5]

There are other pleasing features of the Fourier transforms $R(r)$ for $E_0=E_c$. This can be seen in Fig. 3 where we show $R(r)$ for Fe and Ni for $E_0=E_c$ and for the $E_0=E_{\rm LB}$, the value obtained using Lee and Beni's (LB) criteria[3] and similar to the E_0 values usually used in EXAFS analysis. The latter will be discussed in Sec. V. It is seen in Fig. 3 that the peaks at E_c are much more symmetrical and well defined than those at $E_{\rm LB}$. This is because of the lack of distortion of the peak shapes for the linear phase function. This graphically illustrates that caution should be exercised in analyzing peak shapes from EXAFS. For example

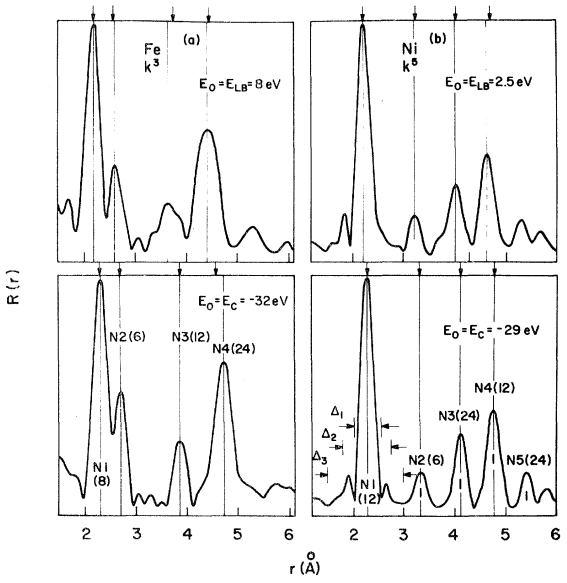

FIG. 3. Radial-scattering distribution obtained by Fourier transforming $\chi(k)$. (a) For Fe with a weighting factor of k^3 and $E_0=E_{\rm LB}=8$ eV and $E_0=E_c=-32$ eV. (b) For Ni with k^5 and $E_0=E_{\rm LB}=2.5$ eV and $E_0=E_c-29$ eV. Note that the distributions obtained with E_c are more symmetrical and well defined. Also the first few shells of each metal have the same shifts in peak position.

at E_{LB} the $N3$ shell in Fe has a definite shoulder which is seen to be an artifact of the analysis since the $N3$ shell shape is entirely symmetrical and well resolved at E_c. Thus the radial transforms obtained using E_c provide much cleaner data for selection of single peaks for back-transformation than those generated from other E_0 values. This removes one source of error in EXAFS data analysis. Another feature that is seen is that the peak shifts for the various shells are similar for E_c but quite different for E_{LB}. In Fig. 3 the vertical arrows indicate the positions of the higher-neighbor shells relative to the $N1$ shell. As seen in Fig. 3, the $N2$ and $N3$ shells of Fe are well aligned for E_c but considerably shifted for E_{LB}. For Ni also, all the peaks are shifted by the same amount for E_c whereas for E_{LB} the $N2$, $N3$, and $N4$ peaks are shifted by different amounts. The shifts for E_{LB} are, of course, also n dependent.

The measured values of E_c for different materials are listed in Tables I—III. They are measured relative to taking the value at the half-height of the step in the absorption curve equal to 0, i.e., $E_K=0$. In cases where there is a sharp excitonic-like peak above the K edge we have also listed the energy relative to this feature in parentheses. We see from the tables that E_c varies from about -30 eV for $Z\sim30$ to positive values for $Z\sim50$. This variation can be related to the systematic variations seen in the phase functions calculated by Teo and Lee.

The values of the shifts in the peak positions, $-\Delta r_i(=b_i/2)$, for these materials with known structure[11] are given in column 4 of Tables I—III. The slopes of the linear variation of peak positions with E_0, $-r_i'=-\Delta r_i/\Delta E_0$ $(=b_i'/2)$, are listed in Tables III—V. Note that although the bond lengths must be known to obtain Δr_i they do not have to be known to obtain r_i' and E_c. Thus, r_i' and E_c can be obtained for any unknown material.

We have found that the difference in r' values for $r\sim2.5$ Å for $n=1$ and 3 is about 0.9×10^{-3} Å/eV. Thus, for materials with $E_c\sim-30$ eV (as Fe to As), this would lead to a difference of about 0.03 Å between analyzing the data with $n=1$ or 3 for $E_0\simeq0$ (the K edge), the value often used.

TABLE II. E_c and E_{LB} values and peak shifts for various compounds (energies in eV and distances in Å).

Compound	E_c	E_{LB}	$-\Delta r_1$	$-\Delta r_{LB}$ $(n=3)$	δr_{LB}	r_n
MnO_2 ($N1$ Mn-O)[a]	−55(−64)	12	0.18	0.35	0.01	1.89
($N2$ Mn-Mn)[b]	−20(−29)	−4	0.23	0.31	0.01	3.426
$FeAs_2$ (Fe-As)[c]	−14	1	0.23	0.27	0.01	2.366
NiAs[d]	−24	1	0.19	0.28	−0.017	2.44
AsNi	−11	10.5	0.27	0.285	−0.02	2.44
$FeGe_2$ (Fe-Ge)[e]	−18	3.5	0.20	0.275	0.00	2.55
NiSe[f]	−13	1	0.24	0.28	−0.01	2.50
$FeSb_2$ (Fe-Sb)[g]	25	0	0.31	0.21	−0.015	2.60
$FeTe_2$ (Fe-Te)[h]	37	−0.5	0.35	0.23	0.00	2.57
NiTe[i]	38	−3	0.39	0.23	−0.03	2.66

[a]2 O at 1.878 Å and 4 O at 1.892 Å.
[b]4 O at 3.345 Å, 8 Mn at 3.426 Å, and 4 O at 3.433 Å.
[c]2 As at 2.327 Å and 4 As at 2.366 Å.
[d]6 As at 2.439 Å and 2 Ni at 2.517 Å.
[e]8 Ge at 2.549 Å and 2 Fe at 2.481 Å.
[f]6 Se at 2.502 Å and 2 Ni at 2.677 Å.
[g]2 Sb at 2.565 Å and 4 Sb at 2.600 Å.
[h]4 Te at 2.562 Å and 2 Te at 2.576 Å.
[i]6 Te at 2.664 Å and 2 Ni at 2.690 Å.

TABLE III. Measured quantities for higher shells for $n=3$.

Material	Shell	E_c (eV)	$-\Delta r_i$ (Å)	a_i (rad)	$-r_i'$ (Å/eV) ($=b_i'/2$) ($\times 10^3$)	a_i' (deg/eV)
Fe	$N1$	−32	0.19	3.4	2.9	7.2
	$N3$	−32	0.20	3.4	5.9	14.8
	$N4$	−31	0.03	5.4	7.7	17.6
Ni	$N1$	−29	0.20	4.4	2.6	6.8
	$N3$	−29	0.18	3.4	5.1	12.6
	$N4$	−29	0.20	6.1	5.4	13.7
Ge	$N1$	−26	0.20	5.8	2.5	6.2
	$N2$	−32	0.11	2.1	4.1	10.8
	$N3$	−15	0.18	5.0	6.2	14.3
Mo	$N1$	−14	0.25	6.8	2.8	7.1
	$N2$	−15	0.26	6.7	2.8	7.9
	$N3$	−15	0.24	5.5	4.3	11.7
Rh	$N1$	0	0.28	8.7	2.4	6.7
	$N3$	0	0.29	9.7	3.9	11.1
	$N4$	−5	0.30	6.7	4.5	12.8
NiAs	$N1$(As)	−24	0.19	5.2	3.5	7.8
	$N4$(As)	−2	0.31	2.5	6.8	14.2

B. Magnitude behavior

The same type of behavior, as seen for the peak positions, is seen in the magnitude of k-independent part a of the phase function. The value of a is obtained by comparing $\mathrm{Im}[R(r)]$ to $|R(r)|$ at the peak positions. To see this, consider only the first shell where $\chi_1(k)$ is given by Eq. (8).

Taking $\phi(k)$ to be linear we substitute χ_i into Eq. (6). Then upon neglecting the variation of the

TABLE IV. Measured quantities for the linear first-neighbor phase functions of some elements at $n=3$.

Element	a_1 a_1 (rad)	a_1' (deg/eV)	$-r_1'$ (Å/eV) ($=b_1'/2$) ($\times 10^3$)	k range (Å^{-1})
^{26}Fe	3.4	7.2	2.9	4–18
^{28}Ni	4.2	6.5	2.6	4–18
^{29}Cu	4.3	7.4	2.5	4–21
^{32}Ge	5.8	6.2	2.5	4–19
^{33}As	6.7	6.75	2.9	4–19
^{34}Se	7.9	6.3	2.4	4–20
^{41}Nb	7.0	7.6	3.1	4–18
^{42}Mo	6.8	7.1	2.8	4–22
^{45}Rb	8.7	6.7	2.4	4–20
^{47}Ag	6.8	7.5	3.0	4–17
^{50}Sn	6.6	8.2	3.2	4–20
^{51}Sb	4.1	8.1	3.3	4–16

TABLE V. Measured parameters of the linear phase functions for various compounds for $n=3$.

Compound	a_1 (rad)	a_1' (deg/eV)	$-r_1'$ (Å/eV) $(=b'/2)$ $(\times 10^3)$	k range (Å^{-1})
MnO_2 ($N1$ Mn-O)	3.1	5.6	2.5	5–16
($N2$ Mn-Mn)	4.95	10.65	4.9	
$FeAs_2$ (Fe-As)	0.50	6.45	2.5	4–18
NiAs	5.2	7.8	3.5	4–15
AsNi	1.1	6.5	2.5	4–20
$FeGe_2$ (Fe-Ge)	5.20	7.72	3.38	4–15
NiSe	0.69	7.1	2.8	4–18
$FeSb_2$ (Fe-Sb)	0.70	8.4	4.06	3.5–15
$FeTe_2$ (Fe-Te)	2.66	7.96	3.55	3.5–16
NiTe	3.4	7.95	3.6	3–15

prefactor compared to that in the exponential terms we get (a procedure similar to that used in Ref. 3):

$$R(r)\simeq\int_{k_1}^{k_2} e^{i\{[2(r-r_i)+b]k-a\}}dk\ , \tag{9}$$

where we have kept only the term with a maximum at positive r. Evaluating Eq. (9) gives

$$|R(r)|\simeq\frac{\sin(k_2-k_1)s}{2s}\ , \tag{10}$$

where $s=r-r_1+b/2$. The peak in $|R(r)|$ is $s=0$ or $r=r_1-b/2$. The imaginary part of $R(r)$ is found to be given by

$$\mathrm{Im}[R(r)]=-|R(r)|\cos[(k_2+k_1)s+a]\ . \tag{11}$$

We can thus obtain the magnitude a at the peak position, $s=0$, from

$$a=\cos^{-1}\{-\mathrm{Im}[R(r)]/|R(r)|\}\ . \tag{12}$$

We obtain $\mathrm{Im}(R)$ because we kept only the positive r values in Eq. (9). In Fig. 2(b) we show the a_i behavior for Ni as a function of E_0. We see that these have a similar behavior to that of the peak positions in that they are essentially straight lines of increasing slope for lower n. They have the same crossover points as the peak position lines and thus can also be used to determine E_c values.

The linear variation of a with E_0 can be understood as follows. For simplicity let us consider the linear phase function which occurs at E_c. Let us also consider only the contribution χ_1 for the first shell. It can be obtained from $R(r)$ by back-transforming as discussed in Sec. IV. At E_c it is of the form

$$\chi_1(k)=-A(k)\sin(2kr_1+a-bk)\ , \tag{13}$$

where the total phase $\Phi(k)=2kr_1+a-bk$. At the nth node in χ_1 we have $\Phi(k_n)=n\pi$, so

$$a_1=n\pi-k_n(2r_1-b)\ , \tag{14}$$

where $k_n=[0.2625(E_n-E_c)]^{1/2}$ and E_n is the energy at the nth node. Energies are in eV and k in Å^{-1}. If we then change from E_c to $E_c+\Delta E$ the momentum at the nth node changes to a new value $\tilde{k}_n=[0.2625(E_n-E_c-\Delta E)]^{1/2}$. Assuming the total phase can still be approximated by a linear function we have $\tilde{\Phi}(k)=2\tilde{k}r_1+\tilde{a}-\tilde{b}\,\tilde{k}$. Again $\tilde{\Phi}(\tilde{k}_n)=n\pi$ so we have

$$\tilde{a}_1=n\pi-\tilde{k}_n(2r_1-\tilde{b})\ . \tag{15}$$

The change in a, $\Delta a=\tilde{a}_1-a_1$ is thus given by

$$\Delta a=2r_1(k_n-\tilde{k}_n)+\tilde{b}\,\tilde{k}_n-bk_n\ . \tag{16}$$

Neglecting the difference between $\tilde{b}$ and b and evaluating $\tilde{k}_n-k_n$ we get

$$\Delta a=0.2625\Delta E(r_1-b/2)/k_n\ ,\qquad a_1'=\Delta a/\Delta E=0.2625(r_1-b/2)/k_n\ . \tag{17}$$

Thus, Δa varies linearly with ΔE as seen in Fig.

2(b). The a' values for many materials are listed in Tables III–V. It can be seen that $a' \sim 7°$/eV or ~ 0.12 rad/eV for $r \sim 2.5$ Å and $n=3$. At the same r value it is $\sim 8°$/eV for $n=1$ and $\sim 6°$/eV for $n=5$. The variation of a' with r can be seen in Fig. 2(b) and Table III. It is obvious that the slope of a_i increases for the higher shells. We found that the k_n values varied between about $4-5$ Å^{-1}, with a tendency for smaller k-range data sets to have lower k_n values. This agrees well with the k_n values calculated by assuming that the dominate nonlinear term in the nonlinear phase functions goes a $1/k$ and linearizing it over the measured k range.

Both $a_i(E_c)$ and a_i' can be uniquely determined for a given atom pair in any material; no knowledge about the structure of the material is required. While $a_i(E_c)$ is independent of n, a_i' is of course n dependent since it involves a weighted average in k. The a_i values are, of course, known only to within multiples of 2π.

C. Slope of peak position variation

As seen in Fig. 2(a), for a given n, the variation of the peak position as a function of E_0 is essentially linear. We define the slope of this linear variation as $r' = -b'/2$. An expression for this slope can be derived in a similar manner to that of the magnitude. In this case we consider the behavior of the total phase $\Phi(k)$ at consecutive nodes k_n and k_{n+1}. Taking the difference of the expressions for the linear phases

$$\Phi(k_{n+1}=(n+1)\pi \text{ and } \Phi(k_n)=n\pi \text{ at } E_c \ ,$$

we obtain

$$b_1 = 2r_1 - \pi/(k_{n+1}-k_n) \ . \tag{18}$$

At $E_c+\Delta E$, where the nodes move to $\tilde{k}_{n+1}$ and $\tilde{k}_n$ we get a similar expression for $\tilde{b}_1$. Taking the difference of $\tilde{b}_1$ and b_1 and substituting in the expressions for $\tilde{k}_{n+1}$ and $\tilde{k}_n$ and keeping terms to first order in $0.2625\Delta E/2k_{n+1}k_n$ we get

$$\Delta b = \tilde{b}_1 - b_1 = 0.2625(r_1 - b/2)\Delta E/k_n k_{n+1} \ ,$$

or defining $b_1' = \Delta b/\Delta E = -2r'$, we get

$$b_1' = 0.2625(r_1 - b/2)/k_n k_{n+1} \ . \tag{19}$$

The r' values for many materials are listed in Tables III–V. It is seen that $r' \sim -2.7\times 10^{-3}$ Å/eV for $r \sim 2.5$ Å and $n=3$. At the same r it is about 0.9×10^{-3} Å/eV more negative for $n=1$ and about 0.6×10^{-3} Å/eV more positive for $n=5$. The variation of r' with bond length can be seen in Fig. 2(a) and Table III, the slope is more negative for greater bond lengths as indicated in Eq. (19). In evaluating Eq. (19), the $(k_n k_{n+1})^{1/2}$ values varied between $\sim 8.5-11$ Å^{-1} with, again, the lower values corresponding to data sets with smaller k ranges and the higher values to sets with larger k range. Again these $(k_n k_{n+1})^{1/2}$ values agree with linearized calculations assuming a $1/k$ term dominates in the nonlinear phase functions. There seems to be no particular correlation between these values and the Debye-Waller factor or energy resolution. The values of k_n and $(k_n k_{n+1})^{1/2}$ are highly correlated with the ratio $(k_n k_{n+1})^{1/2}/k_n$ being between 2.1 and 2.3 for $n=3$.

Thus we can understand the behavior of all the features seen in Fig. 2. For any material the procedure described here gives a method to obtain E_c and the quantities $r_1 - b/2$, a, a', and b' which characterize the linear phase function and its variation with E_0. We can further investigate the behavior of the phase functions by back-transforming $R(r)$ and deriving the amplitude and phase functions by use of Eq. (1).

IV. BACKTRANSFORMING THE DATA

A further step often used in analyzing EXAFS data is to obtain the individual contributions χ_i by back-transforming the individual peaks of the radial scattering function $R(r)$. That is

$$\chi_i(k) = \sqrt{2/\pi} \int_{r_0}^{r_u} R(r) e^{-2ikr} dr \ , \tag{20}$$

where r_0 and r_u are values spanning the peak due to the ith shell. Considering the first shell we have

$$\chi_1(k) = \mathrm{Re}(\chi_1) + i\,\mathrm{Im}(\chi_1) = |\chi_1| e^{i\Phi_1(k)} \ , \tag{21}$$

where

$$\chi_1 = \frac{N_1}{kr_1^2} |F_1| e^{-2\sigma_1^2 k^2} e^{-2r_1/\lambda_1} W(k) k^n \ , \tag{22}$$

and

$$\Phi_1(k) = 2kr_1 + \phi_1(k) = \cos^{-1}[\mathrm{Im}(\chi_1)/|\chi_1|] \ . \tag{23}$$

Where $\mathrm{Im}(\chi_1)$ occurs because we retain only positive r values in the Fourier transforms.

$|\chi|$ thus contains information about N, F, σ, and λ. In practice the shape of the scattering function, especially at low k values, is sensitive to the values r_0 and r_u and to the value of n used in the Fourier transforms. This is shown in Fig. 4 where we show $F_1(\pi,k)e^{-2r_1/\lambda_1}$ for various (r_0,r_u) regions as indicated for Ni in Fig. 3(b) by Δ_1, Δ_2, and Δ_3. This sensitivity can make evaluation of quantities in the prefactor somewhat subjective. The calculated F values of Teo and Lee[5] are typically a factor 1.7—2.0 times larger than the derived values of $F_1e^{-2r_1/\lambda_1}$ values for an interval such as Δ_2. Part of this is due to inelastic scattering as represented by the factor e^{-2r_1/λ_1}. Inelastic and multiple scattering, as well as many-body and thickness effects must be considered in evaluating the quantities in the prefactor. Discussions of some of these difficulties have been published recently.[6,7] Amplitude transferability is found to hold only for chemically similar materials, so that coordination number determinations can be quite inaccurate.[7] In this paper we will not consider the amplitude and prefactors any further but will concentrate on the simpler determination of bond lengths. In contrast to the sensitivity of the prefactor parameters to the (r_0,r_u) interval, the phase functions $\phi(k)$ obtained by back-transforming are essentially insensitive to the tails of well-resolved peaks.

A. Determination of phase functions

The phase functions $\phi(k)$ of an atom pair in a material whose structure is known can be determined from Eq. (23) which relates k (and thus, E_0), r_i, and ϕ. The $\phi(k)$ functions vary systematically as E_0 is varied. This is shown in Figs. 5 and 6(a) where we show typical sets of phase functions of the first shells of Ni and Ge for various E_0 values. We see that the phase functions are sets of curves that tend to converge at high k values and fan out at low k values due to the slopes being increasingly negative as E_0 increases. It can be seen that, as expected, the $\phi(k)$ curves for $E_0=E_c$ (-29 eV for Ni and -26 eV for Ge) are linear. The dashed curves are the phase function calculated by Teo and Lee.[5] In Fig. 7(a) we show the derived $\phi(k)$ for the well-defined $N1$, $N3$, and $N4$ peaks of Ni for E_c. $N2$ is left out since it is too small to give a reliable peak due to having only six sites. We see that all shells have similar slopes, b, as was already evident in Fig. 3 where all the peaks were shifted by the same amount. However, the magnitudes a, are seen to be different for the various shells. In Fig. 7(b) we show the derived $\phi(k)$ functions for $N1$, $N3$, and $N4$ evaluated for the E_0 value (2.5 eV) determined by the Lee and Beni procedure.[3] We see that for this E_0 value the $\phi(k)$ have different slopes as was also seen in the peak positions in Fig. 3(b). They also have different magnitudes.

In Fig. 6 we show the derived linear $\phi(k)$ functions for the $N1$, $N3$, and $N4$ shells of Ge at their respective E_c values. This nonmetal not only has different E_c values for the different shell but also different slopes (although $N1$ and $N3$ are similar) and a values. Thus we have found that there is no phase transferability between shells for this nonmetal.

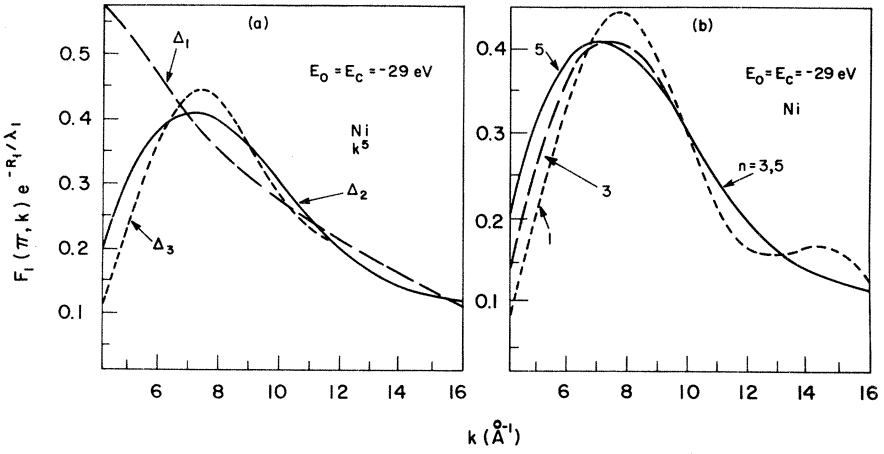

FIG. 4. Derived amplitude functions of Ni, (a) for a k^5 weighting factor and the various r regions Δ_1, Δ_2, and Δ_3 as shown in Fig. 3(b), (b) for the interval Δ_2 for different weighting factor k^1, k^3, or k^5.

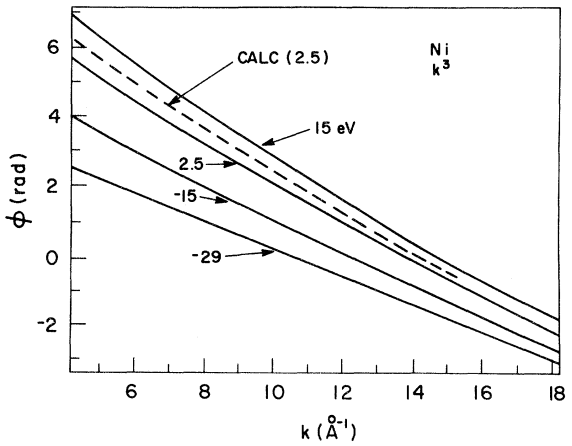

FIG. 5. Derived phase functions $\phi(k)$ for various E_0 values for the $N1$ shell of Ni. The linear $\phi(k)$ is obtained at $E_0=E_c=-29$ eV. The dashed curve is the Ni phase function calculated in Ref. 5. It corresponds to $E_{LB}=2.5$ eV as described in the text.

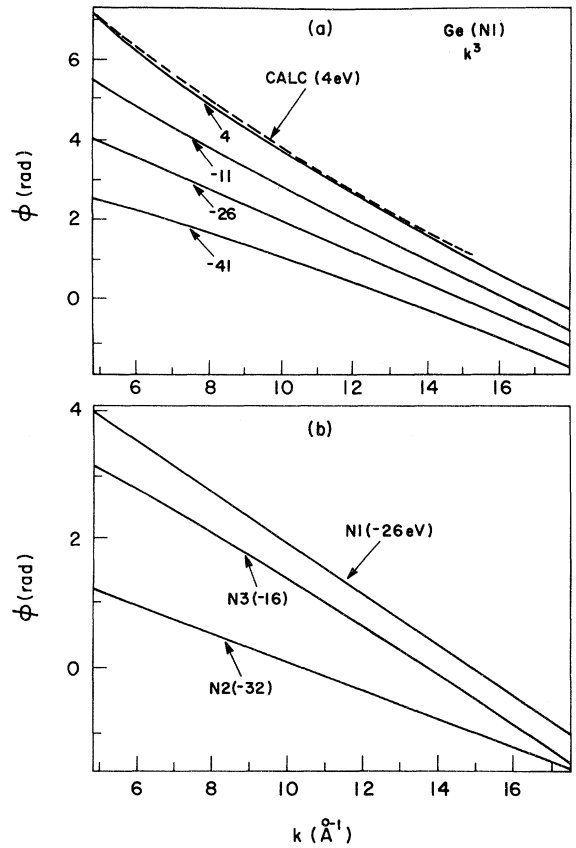

FIG. 6. Derived phase functions $\phi(k)$ for Ge. (a) the variation of $\phi(k)$ for the $N1$ shell for various E_0 values. The linear $\phi(k)$ corresponds to $E_c=-26$ eV. The dashed curve is the phase function calculated in Ref. 5. (b) The $\phi(k)$ functions for the first three shells for their respective E_c values. Note that in this nonmetal the E_c values and slopes are different for the first three shells.

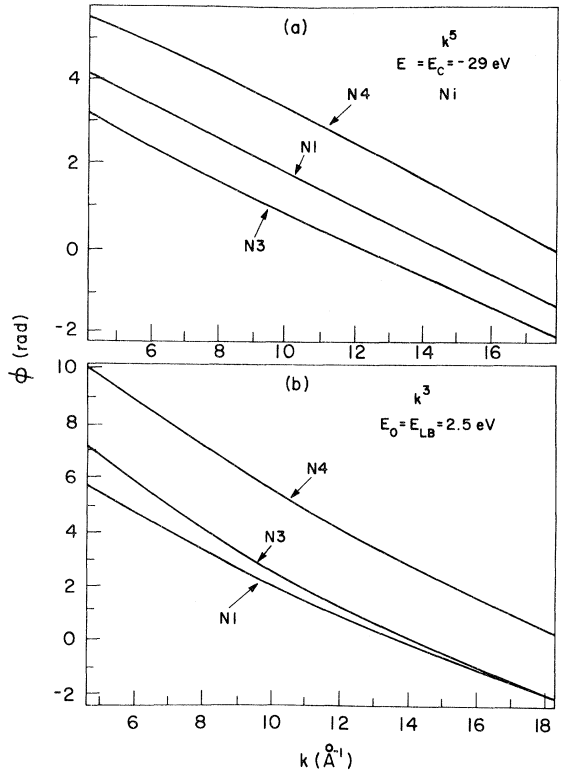

FIG. 7. Derived phase functions $\phi(k)$ for the $N1$ $N3$, and $N4$ shells of Ni. (a) $E_0=E_c=-29$ eV, note that they all have essentially the same slope but different magnitudes. (b) $E_0=E_{LB}=2.5$ eV, the slopes as well as magnitudes are no longer the same for the different shells.

It should be emphasized that the $a(E_0)$ curves such as shown in Fig. 2(b) are not the intercepts of the derived $\phi(k)$ curves as seen in Figs. 5 and 6(a) (the $\phi(k)$ are actually never determined below $\sim 3-4$ Å^{-1}) but are values corresponding to replacing each $\phi(k)$ curve by the linear approximation $\phi(k)=a_{\text{eff}}-b_{\text{eff}}k$.

In Tables I–V we have listed the parameters characteristic of the materials measured. We see that the $\phi(k)$ at any energy, $E_0=E_c+\Delta E$ can be represented in terms of the linear $\phi(k)$ at E_c by

$$\phi(E_0)=\phi(E_c)+(a'-b'k)\Delta E\ , \tag{24}$$

or $\Delta\phi=\phi(E_0)-\phi(E_c)$, is given by

$$\Delta\phi=(a'-b'k)\Delta E\ , \tag{25}$$

where $b'=-2r'$. It is of interest to compare this to the usual expression for $\Delta\phi$ used in the literature.[3] This is obtained by setting $\Delta\phi=2r\Delta k$ so from Eq. (7),

$$\Delta\phi=0.2625r\Delta E/k\ . \tag{26}$$

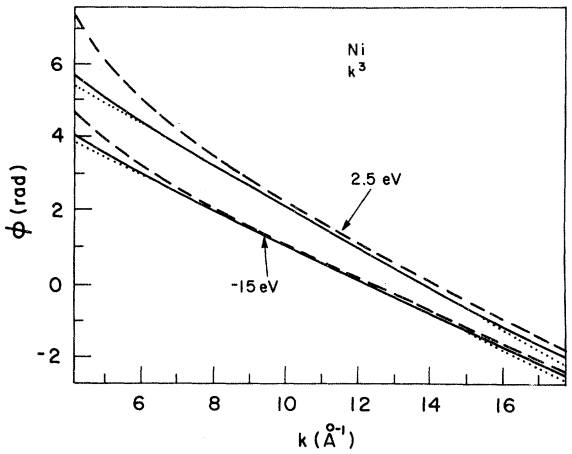

FIG. 8. The "true" back-transformed $\phi(k)$ for Ni at $E_0=-15$ and 2.5 eV are shown by the solid curves. The other curves are derived from the linear phase function obtained at $E_0=-29$ eV using two different procedures as discussed in the text.

In Fig. 8 we show $\phi(k)$ functions for Ni calculated using Eqs. (25) and (26) for $E_0=-15$ and 2.5 eV starting with the linear $\phi(k)$ at $E_c=-29$ eV. The solid curves are the "true" $\phi(k)$ obtained by back-transforming with $E_0=-15$ and 2.5 eV. The dashed curves are those obtained using Eq. (26) and the dotted curves are obtained using Eq. (25). The linear approximation, Eq. (25), is seen to fit the derived $\phi(k)$'s much better than that obtained with Eq. (26). A better approximation than Eq. (26) is made by using the more correct form

$$\Delta\phi=(2r-b)r\Delta E/k\ , \tag{27}$$

but this requires knowing b and still gives a poor fit at low k (<6 Å^{-1}) compared to the linear approximation.

As seen from the derived $\phi(k)$ functions in Figs. 5 and 6(a), an atom pair in a given material can be equally well represented by any of a continually varying family of $\phi(k)$ curves. We can well ask if there is any unique E_0 value which is characteristic of the material? There seems to be no reason for this to be so. Thus we take the point of view that all the $\phi(k)$ represent the atom pair equally well. This being so, it is of great advantage to use E_c and its accompanying linear $\phi(k)$ to represent the material. We can simply regard E_c as being a parameter which selects the pseudopotential of the crystal that gives rise to only s-wave scattering of the photoelectrons. This pseudopotential can be thought of as a square well of width $b/2$ and whose depth is related to the k-independent magnitude, a. Thus, in a metal, where all the shells have the same E_c value, the similar b values would indicate that the size of the atoms are the same in all direction or the potentials are isotropic. However we found that at E_c in a metal the magnitudes or well depths were usually unequal for the different shells or directions. In nonmetals we found that the E_c values were different for different shells indicating that the size or potentials of the atoms look different in different directions.

Having obtained the linear $\phi(k)$, we see from Fig. 8 that is is reasonable to use linear expansions to examine the behavior of the phase functions. In particular it is of interest to consider various relations of the $\phi(k)$ function for the same atom pair in two different materials A and B.

V. RELATIONS BETWEEN FAMILIES OF PHASE FUNCTIONS

As shown in Sec. III, for a known structure, the quantities E_c, a, b, a', and b' can be uniquely determined. Thus suppose we have determined the families of phase functions $\phi_A(k)$ and $\phi_B(k)$ for the same atom pair in materials A and B. We can then consider various possible cases. First let us consider the case where the two families contain an identical pair of phase functions.

A. An identical pair of phase functions (phase transferability)

Suppose two of the families of phase functions are the same for two E_0 values, say E_A and E_B, that is, $\phi_A(E_A)=\phi_B(E_B)$. We want to know if there are any other matched pairs for shifts in E_0 of ΔE_A and ΔE_B. Considering phase functions in the vicinity of the linear ϕ we can use the linear approximation and determine the conditions necessary to have other matched pairs.

Using Eq. (24) we obtain that the relation between the new pair is

$$(a'_A-b'_Ak)\Delta E_A=(a'_B-b'_Bk)\Delta E_B\ . \tag{28}$$

Using Eqs. (17) and (19) for a' and b' we see that Eq. (28) requires that ΔE_A and ΔE_B are related by

$$\Delta E_B/\Delta E_A=(r_A-b_A/2)s_A/(r_B-b_B/2)s_B\ , \tag{29}$$

where $s=1/\langle k_n\rangle-k/\langle k_nk_{n+1}\rangle$. If the k ranges are matched so that $\langle k_n\rangle$ and $\langle k_nk_{n+1}\rangle$ are the same in A and B, the energy shifts are in the same ratio as the transformed peak positions. If the k

ranges are not the same $\langle k_n \rangle$ and $\langle k_n k_{n+1} \rangle$ for A and B are different and the left-hand side of Eq. (29) becomes k dependent. Thus, the procedure often used, of finding the phase function of a known material at an arbitrary E_0 (generally near the K edge) and then using it to generate $\phi(k)$ at other E_0 values, is valid only if the k ranges of the A and B data sets are the same. Furthermore, as we saw in Fig. 8 the usual method of deriving one phase function from another, using $\Delta\phi = 2r\Delta k$, is not very accurate.

B. No matching phase functions

Conversely if one phase function in material A has no identical corresponding phase function in B, then none of the $\phi(k)$'s coincide. There are two convenient ways to consider the mismatch: the slopes matching but not the magnitudes and the inverse. These are equivalent, alternate ways to match the sets of phase functions.

1. Matching slopes

In this case we have $b_A(E_A) = b_B(E_B)$ and $a_A(E_A) \neq a_B(E_B)$. In a similar procedure to that used above we find that while the magnitudes at E_A and E_B were separated by $a_B(E_B) - a_A(E_B)$, those at $E_A + \Delta E_A$ and $E_B + \Delta E_B$ are separated by

$$\Delta a = a_B(E_B) - a_A(E_A) + a'_A \Delta E_A (t_B/t_A - 1) ,$$

where $t = \langle k_n k_{n+1} \rangle / \langle k_n \rangle$. If the k ranges are matched so that $\langle k_n \rangle$ and $\langle k_n k_{n+1} \rangle$ have the same value in both materials, then each pair of phase functions having the same slope is separated by Δa in magnitude. So, in this case, there are no identical $\phi(k)$ in the two sets. Since only the slope, or b value, determines the peak position, a match of this type will give the correct bond length. In fact this is the type of matching seen between shells in metals at E_c as seen in Fig. 7 for Ni where the slopes, or peak shifts, are all the same but the a values are different.

2. Matching magnitudes

In this case we have $a_A(E_A) = a_B(E_B)$ and $b_A(E_A) \neq b_B(E_b)$. Here we find that the difference in slopes between phase functions at $E_A + \Delta E_A$ and $E_B + \Delta E_B$ is given by

$$\Delta b = b_B(E_B) - b_A(E_A) + b'_A \Delta E_A (t_A/t_B - 1) .$$

For $\langle k_n \rangle$ and $\langle k_n k_{n+1} \rangle$ being the same in the two materials the difference in slopes are the same for all pairs of phase functions having the same a values.

Under the circumstance of having the values of $\langle k_n \rangle$ and $\langle k_n k_{n+1} \rangle$ the same for the two different materials the relation between pairing the sets in any manner is always $\Delta E_A / \Delta E_B = (r_A - b_A/2)/(r_B - b_B/2)$, whether phase transferability exists or not.

VI. PROPOSED METHOD TO EVALUATE BOND-LENGTH USING LINEAR PHASE SHIFTS

We propose a procedure for determining bond lengths which should be simpler, more objective, and more accurate than other methods in use. Until a library of linear phase functions is accumulated, it requires using model compounds as do the other methods in use. The procedure is as follows.

The measured $\chi(k)$ of a given atom pair is analyzed as described in Sec. III and the quantities E_c, a, a', and b' are determined from plots such as shown in Fig. 2 for both the known A and unknown material B. The n-independent quantity $b_A(E_c^A)$ is also obtained for the known material A. For the unknown material the corresponding quantity $r_m = r_B - b_B(E_c^B)$ is obtained. The energy shift ΔE_B $(= E_B - E_c^B)$ which equates the magnitude $a_B(E_B)$ to the measured magnitude $a_A(E_c^A)$ is obtained from the linear approximation to be

$$\Delta E_B = [a_A(E_c^A) - a_B(E_c^B)]/a'_B . \tag{30}$$

The magnitudes of the nonlinear phase functions are difficult to determine accurately in contrast with those of the linear $\phi(k)$. The linear $\phi(k)$ are furthermore least k-range dependent.

If there is phase transferability, then $b_B(E_c^B + \Delta E_B) = b_A(E_c^A)$, and the desired quantity, $b_B(E_c^B)$, needed to determine the bond length is given by

$$b_B(E_c^B) = b_A(E_c^A) - b'_B[a_A(E_c^A) - a_B(E_c^B)]/a'_B . \tag{31}$$

The bond length is then obtained by adding $b_B(E_c^B)$ to the measured peak position at $E_0 = E_c^B$ of material B. In Sec. III we found that a' and b' are somewhat k-range dependent. However we also found that their ratio was quite unsensitive to the

k range and fortunately it is the ratio which enters the bond-length determination. In this method no back-transforms need be taken, only the peak positions as a function of E_0 for various n values are required. However, it is often of interest to derive $\phi(k)$ by back-transforming to check on its linearity.

Unless the calculated components ϕ_a and ϕ_b that now exist in the literature are linearized they are of no use for the method described here. One considerable advantage of the linear $\phi(k)$ is that they can be characterized by five numbers rather than require a table of values.

The question of the validity of phase transferability is under continual investigation. As seen from Tables I and II, and other determinations in the literature, bond lengths can be reliably determined to about 1% or 0.03 Å at the present time. More accurate determinations on known structures are often obtained[12,13] but this may be because the criteria involved in the analysis procedures are subjective enough that if the bond length is known it can be obtained. On the other hand, for an unknown material it is difficult to judge the accuracy of a given determination. We now discuss and compare some of the other methods of analysis.

VII. DISCUSSION OF OTHER METHODS OF ANALYSIS

There have been several methods of analysis proposed in the literature. All assume phase transferability and use phase functions which are either calculated or determined from model compounds of known bond lengths containing the same atom pairs. We will first discuss a technique due to Lee and Beni[3] (LB) which is really a procedure to test the validity of calculated $\phi(k)$ functions for a known material.

A. Lee and Beni procedure

The procedure proposed by LB is to calculate $R(r)$, in a manner similar to that given by Eq. (6), but with the phase function and the inverse of the prefactor in $\chi_1(k)$ included in the integrand so that their effects are eliminated. Thus, in Eq. (6) $\chi(k)$ is divided by the prefactor in Eq. (1) and a factor $e^{i\phi(k)}$ is included in the integrand. $R(r)$ is then calculated for various E_0 until $\mathrm{Im}(R)$ and $|R|$ peak at the same r value. If this r value corresponds to the known bond length for a particular atom pair it shows that the phase function being used is one of the set that represents the material under consideration and that the magnitude a and the slope b are properly correlated.

The derivation[3] of this criteria, $\mathrm{Im}(R)$ and $|R|$ peaking at the same place, assumes that the phase is linear. Nonlinear terms would lead to extra terms in the integral and a more complex criteria. Thus the curved $\phi(k)$ is effectively replaced by $\phi(k)=a_{\mathrm{eff}}-b_{\mathrm{eff}}k$ in obtaining the LB criteria.

Using this procedure we have obtained the E_0 values, called E_{LB}, for the nearest-neighbor shells. They are listed in Tables I and II. As seen in Table I, the E_{LB} values for the elements are in the range 0 ± 8 eV. This is a result of the potentials used by Teo and Lee.[5] In Tables I and II we also list the deviation δr_{LB}, of the peak position from the known radial distance. We see that there is fair agreement, usually within 0.02 or 0.03 Å, for most of the elements examined in this work. However the δr_{LB} value for Ag is -0.10 Å, indicating that the phase shifts for this element listed by Teo and Lee (TL) are not good. An inspection of the values for Ag in Ref. 5 shows that its $\phi(k)$ is indeed anomalous compared to those near it. The phase functions obtained in the TL calculation are, of course, not unique. Any of the family of $\phi(k)$ curves, typically shown in Figs. 5 and 6(a), would meet the LB criteria and give the correct radial distance. In Figs. 5 and 6(a) we show the calculated TL phase shifts by the dashed curves. We see that they give fair fits to the measured $\phi(k)$ at E_{LB} although for Ni there is a displacement by about 6 eV. In general the measured $\phi(k)$ show less curvature and structure at low k than the calculated $\phi(k)$ in Ref. 5. The obvious advantage of using the calculated phase shifts is that the individual contributions from the absorber ϕ_a and the scatterer ϕ_b can be obtained for all elements and then combined in any combination to give the phase shifts due to any atom pair. As we shall show later these individual components cannot be determined experimentally.

In Tables I and II we have also listed the $N1$ peak position shifts, $-\Delta r_{\mathrm{LB}}$, for $R(r)$ as given by Eq. (6) with $E_0=E_{\mathrm{LB}}$ and a weighting factor of $n=3$. We see that, for the elements investigated here, these shifts vary between 0.26 and 0.35 Å. The similar peak shifts of the linear phase functions are seen to vary between 0.20 and 0.38 Å. The LB procedure could also obviously be used with $\phi(k)$ that are obtained experimentally from a

model compound of known structure containing the same atom pair.

B. Method of constant r

This method was proposed by Martens *et al.*[12] Here one uses either a calculated phase function or one that is obtained from a known material A by back-transforming to get $\chi_1(k)$ as described in Sec. IV, Eq. (23). E_0 is usually assumed to be near the K edge. Since r_A is known the phase function is thus determined within a factor of $2\pi n$ by

$$\phi_A(k,E_0)=\Phi_A(k,E_0)-2kr_A \ .$$

For the same E_0 the total phase Φ_B, of a second material with the same atom pair, is determined by back-transforming. The bond length in B is then obtained by

$$r_B(k,E_0)=[\Phi_B(k,E_0)-\phi_A(k,E_0)]/2k \ .$$

This r_B generally varies considerably with k, so E_0 is then changed and the procedure repeated until the derived bond length

$$r_B(k,E_0+\Delta E)=[\ \Phi_B(k,E_0+\Delta E) -\phi_A(k,E_0)]/2k \ , \tag{32}$$

becomes constant over a large region of the k range.

Considering the phase functions as linearized, with effective magnitudes and slopes, the method is essentially equivalent to the LB procedure. By requiring that r_B be constant the magnitudes, a_{eff}, are matched since for a linearized phase Eq. (32) becomes

$$r(k,E_0+\Delta E)=r_B+[a^B_{\text{eff}}(E_0+\Delta E)-a^A_{\text{eff}}(E_0)]/2k -[b^B_{\text{eff}}(E_0+\Delta E)-b^A_{\text{eff}}(E_0)] \ .$$

Both methods A and B are seen to be procedures to minimize the $1/k$ terms in the phase functions. Note that if there were not phase transferability, or the known phase function were in error, these methods are similar to those in Sec. IV B 2, where the magnitudes are matched and the slopes are not equal. The resulting bond length would be in error by the difference of the effective slopes of the phase functions for A and B.

C. Matching total phases at $k=0$

This is a similar procedure[13] to the constant r method. It differs in that it uses the total back-transformed Φ_A and Φ_B and matches them at $k=0$ by varying the E_0 of the unknown B. As can be seen from Eq. (23) this again matches the a_{eff} values. Both methods B and C effectively linearize the usually curved $\phi(k)$. The method proposed here in Sec. VI has the advantage that it starts out with a linear $\phi(k)$.

D. Least-squares fit to $\chi(k)$

In this method a trial χ_T is obtained using calculated or derived amplitude and phase functions in the theoretical expression given in Eq. (1). This χ_T is compared to the experimental, back-transformed χ_E (derived for a fixed E_0^E) using a least-squares procedure (e.g., SIMPLEX). E_0^T, r_1 and as many other parameters of Eq. (1) as desired are varied. Usually E_0^E is set equal to zero at the K edge and the change in $\phi(k)$ with E_0^T is taken as $\Delta\phi=0.2625r\Delta E/k$. As we saw in Fig. 8 and its discussion, this is not a very good approximation to $\Delta\phi$. It is much better to use $\Delta\phi=0.2625\times(r-b_{\text{eff}})\Delta E/k$ or the $\Delta\phi$ given by the linear approximation in Eq. (25).

We have found that the bond lengths obtained using this method often vary with the number and choice of parameters. Although the parameters in the prefactor of Eq. (1) are not strongly coupled to the argument of the sine there is some coupling. It is difficult to judge the accuracy of bond lengths determined by this method.

VIII. DERIVATION OF GENERAL PHASE TRANSFERABILITY

We have shown that for each atom pair there exists a set of phase functions $\phi(k,E_0)$, parameterized by E_0 values, all of which equally well represent the phase function of the atom pair. We have also found that one of this set of phase functions, $\phi_l(k,E_c)$, is linear and we characterize its E_0 value by E_c. Bond lengths are determined most accurately by working in the vicinity of $\phi_l(k,E_c)$. A further advantage of using ϕ_l and linearizing the set of $\phi(k)$ as described in Sec. IV, is that the assumption of phase transferability can be easily examined.

In a narrow sense, phase transferability assumes that the same set of $\phi(k)$ applies to a given atom pair no matter what the environment of that pair

and that the different environments can be described by relabeling the E_0 values of the $\phi(k)$'s. Thus, in practice, the environmental changes are taken into account by varying the "muffin-tin zero" which is characterized by the value of E_0. The method of analysis proposed in Sec. VI, and in general all methods of analysis, obtain the change in E_0 by equating the magnitudes, a.

There is a more general type of phase transferability between different atom pairs. These interdependences have often been referred to in the literature;[14] but in a rather obscure manner since it has not been understood how to select the E_0 values to be used in the comparison of the various atom pairs. Only by using the linearized $\phi(k)$ can this problem be easily addressed. General transferability thus assumes that there are relations between phase functions of the type

$$\phi_{AB}+\phi_{CD}=\phi_{AD}+\phi_{CB} , \tag{33}$$

where C and D could be A or B. The type of transferability represented by Eq. (33) is very important since it reduces the number of phase functions needed to completely represent a system of N different elements to $2N-1$ rather than N^2 which would be necessary if no such relations existed.

It should be pointed out that the individual absorber and backscatterer functions can never be derived experimentally. If we have a system with N different atoms then, assuming dependencies as given by Eq. (33), the number of independent measurable quantities is $2N-1$. However there are $2N$ independent unknown functions involved, two for each type atom. Thus, we can never obtain the $2N$ unknowns. We could, of course, arbitrarily define one phase function and obtain all the others relative to it.

The difficulty to the present time, in using relations as given by Eq. (33) has been the question of which values of E_0 should be used. We give a procedure to determine these relevant E_0 values. It is analogous to the procedure used in applying phase transferability in the narrower sense, i.e., the E_0 values are obtained by setting all the magnitudes, a, to be equal. (The E_0 values could equally well be obtained by setting the slopes, $b/2$, equal.) Thus, e.g., we could obtain the desirable E_0 values by setting all the a values equal to $a_{AB}(E_c^{AB})$ where

$$\phi_{AB}(k,E_c^{AB})=a_{AB}(E_c^{AB})-b_{AB}(E_c^{AB})k .$$

We can then find the E_0 value, E_{CD}, for the CD materials by using Eq. (24). We get

$$E_{CD}=[a_{AB}(E_c^{AB})-a_{CD}(E_c^{CD})]/a'_{CD}+E_c^{CD} . \tag{34}$$

Note that all quantities on the right side of Eq. (34) can be measured. The value of E_{AD} and E_{CB} can be similarily derived. The more explicit form of Eq. (33) is thus,

$$\phi_{AB}(k,E_c^{AB})+\phi_{CD}(k,E_{CD}) = \phi_{AD}(E_{AD})+\phi_{CB}(E_{CB}) . \tag{35}$$

We can now test the more general transferability by seeing whether

$$b_{AB}(E_c^{AB})+b_{CD}(E_{CD})=b_{AD}(E_{AD})+b_{CB}(E_{CB}) , \tag{36}$$

where

$$b_{CD}(E_{CD})=b_{CD}(E_c^{CD}) +[a_{AB}(E_c^{AB})-a_{CD}(E_c^{CD})]b'_{CD}/a'_{CD} , \tag{37}$$

and similarily for $b_{AD}(E_{AD})$ and $b_{CB}(E_{CB})$. The results of testing Eq. (36) for $\phi_{\mathrm{NiNi}}+\phi_{\mathrm{AsAs}}=\phi_{\mathrm{NiAs}}+\phi_{\mathrm{AsNi}}$ and $\phi_{\mathrm{FeAs}}+\phi_{\mathrm{NiTe}}=\phi_{\mathrm{FeTe}}+\phi_{\mathrm{NiAs}}$ are shown in Table VI. We see that for the Ni-As system the sum of the peak position shifts is the same within 0.001 Å. For the Fe-Ni-As-Te system the $b/2$ sums are the same to within 0.02 Å. It is expected that materials of similar atomic number such as Ni and As would have general transferability. A more rigorous test of the transferability involves atoms of widely different Z and bonding. Thus the difference of 0.02 Å in the $b/2$ sums for the Fe-Ni-As-Te system may be real or just due to inaccuracies, e.g., due to different k ranges of the

TABLE VI. Test of general transferability.

Elements					
A	B	C	D	$\frac{1}{2}[b_{AB}(E_c^{AB})+b_{CD}(E_{CD})]$	$\frac{1}{2}[b_{AD}(E_{AD})+b_{CB}(E_{CB})]$
Ni	Ni	As	As	0.503A	0.502A
Fe	As	Ni	Te	0.505A	0.525A

data. Further tests of transferability are in progress.

In reality the E_{CD}, E_{AB}, and E_{CB} values never have to be evaluated since as seen in Eq. (37) the b values can be obtained from the measured quantities $a(E_c)$, $b(E_c)$, b', and a'. As in Eq. (31) only the ratio b'/a', which is quite insensitive to the k range of the data and should be a constant for equal k ranges, enters in the evaluation of the general transferability relations. It can be shown that all the a values do not have to be taken equal. It is sufficient that just the sums of the a values on the two sides of Eq. (36) be made equal. As long as the ratios b'/a' are equal, which they are for good data of similar k range, taking arbitrary a values, but of equal sums, on the two sides of Eq. (36) can be shown to be equivalent to taking all the a values equal. Thus, any one of the ϕ functions in Eq. (35) can be entirely derived from the other three ϕ functions by using the procedures described above. So, in principle, only $2N-1$ phase functions need be measured to completely characterize all the possible pairs in a system of N element.

IX. SUMMARY

The advantages in using the linear phase functions, rather than those derived at some arbitrary E_0 are that they are much easier to use and manipulate. Since most of the other analysis methods essentially involve linearizing the phase functions it is more accurate to determine and use the linear functions directly. The amount of work involved in processing the data is no greater than for the other methods. With the linear method one Fourier transform is made for a few E_0 values for $n=1$, 3, and 5. For the other methods a series of Fourier-transforming and back-transforming for various E_0 values is required until some criteria on E_0 is met. Further advantages of using the linear method are as follows.

(1) The E_c, a, $r_i-b/2$, a', and b' values can be uniquely determined for each material.

(2) The analysis is independent of the weighting factor n.

(3) Much cleaner looking $R(r)$ spectra are obtained at E_c than other E_0 values due to reduced distortion of peaks. This is especially so for metals where the E_c values tend to be the same for the first few shells.

(4) The quality of the data can be assessed from whether or not a crossover point exists. In fact this provides a good criteria for identifying spurious peaks.

(5) For metals the slopes of the phase function or peak positions are found to be the same at E_c.

Using linear phase functions removes the subjectivity involved in the other methods of analysis. For good data sets that fulfill the criteria described above it appears to be possible to determine bond lengths in unknowns to about $0.01-0.02$ Å. Furthermore, using the methods described here the accuracy of the inter-relations between the phase functions of pairs of different atoms can be tested.

ACKNOWLEDGMENTS

I would like to thank F. W. Lytle for providing many of the data tapes and collaboration in obtaining much of the data. I would also like to thank F. Fradin and B. Kincaid for providing me with tapes of their EXAFS programs. I am grateful to D. G. Stearns and S. Laderman for many discussions concerning EXAFS. Data were taken using the facilities of SSRL at Stanford and CHESS at Cornell and I thank the staffs of both for their considerable aid and hospitality throughout the course of my runs.

---

*Present address: Department of Physics, Arizona State University, Tempe, Arizona 85287.

[1]F. W. Lytle, D. E. Sayers, and E. A. Stern, Phys. Rev. B 11, 4825 (1975).

[2]E. A. Stern, Phys. Rev. B 10, 3027 (1974).

[3]P. A. Lee and G. Beni, Phys. Rev. B 15, 2862 (1977).

[4]C. A. Ashley and S. Doniach, Phys. Rev. B 11, 1279 (1975).

[5]B. K. Teo and P. A. Lee, J. Am. Chem. Soc. 101:11, 2815 (1979).

[6]E. A. Stern, B. A. Bunker, and S. M. Heald, Phys. Rev. B 21, 5521 (1980).

[7]P. Eisenberger and B. Lengeler, Phys. Rev. B 22, 3551 (1980).

[8]R. B. Greegor and F. W. Lytle, Phys. Rev. B 20, 4902 (1979).

[9]B. Lengeler and P. Eisenberger, Phys. Rev. B 21, 4507 (1980).

[10]*International Tables for X-ray Crystallography* (Kynoch, Birmingham, England, 1962), Table 3.2.2c,

p. 171.
[11]Distances were obtained from W. B. Pearson, *A Handbook of Lattice Spacings and Structures of Metals and Alloys* (Pergamon, New York, 1967), Vol. 2; J. Donohue, *The Structure of the Elements* (Wiley, New York, 1974); R. W. G. Wyckoff, *Crystal Structures* (Interscience, New York, 1958), Vol. 1.
[12]G. Martens, P. Rabe, N. Schwenter, and A. Weiner, Phys. Rev. B 17, 1481 (1978); P. Rabe, Jpn. J. Appl. Phys. 17-2, 22 (1978).
[13]P. A. Lee, B. M. Citrin, P. Eisenberger, and B. M. Kincaid, Rev. Mod. Phys. 53, 769 (1981).
[14]P. H. Citrin, P. Eisenberger, and B. M. Kincaid, Phys. Rev. Lett. 36, 1346 (1976).